Propagation factors influencing observations of resonances of atmospheric gravity waves

Nikolay Zabotin[1] and Oleg Godin[2]

[1] Department of Electrical, Energy and Computer Engineering, University of Colorado, Boulder
[2] Department of Physics, Naval Postgraduate School, Monterey, CA

EGU 2020 Online Session, 8 May 2020

© Authors. All rights reserved

Outline

1. Observational evidences of atmospheric resonances
   - "acoustic resonances" in the atmosphere
   - manifestations of resonances in GWs radiated by the ocean
2. A glimpse of the unified theory of atmospheric resonances
3. Relationship between full-wave and WKB solutions for acoustic resonances
4. Excitation of resonant and non-resonant atmospheric waves by vibrations of the ground and ocean surfaces
5. Propagation properties of buoyancy resonances in a mid-latitude atmosphere
6. Diversity of resonance conditions for gravity waves radiated by the ocean in mid latitudes
7. Relationship between full-wave and WKB solutions for buoyancy resonances
8. Bathymetry of north-west Atlantic and correlation of the oceanic and atmospheric wave activity observed in the area

Atmospheric acoustic resonances

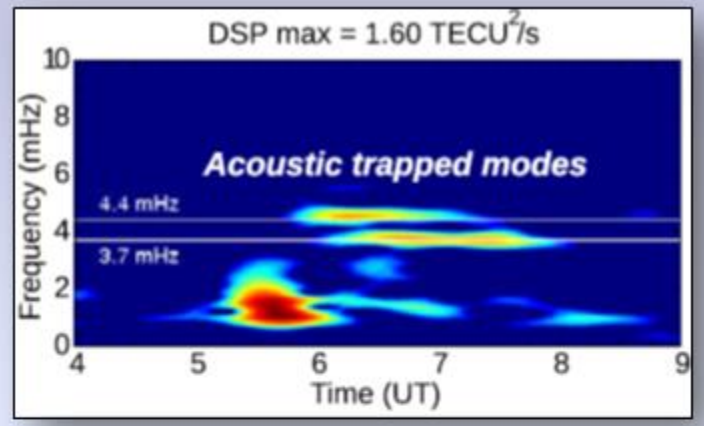

Spectrogram of STEC observations after Tohoku earthquake [Rolland, L.M., Lognonné, P., Astafyeva, E. et al., Earth Planet Sp., 2011, Fig. 3a]

- Are caused by wave reflection in mesopause
- Are found in the range 3.7–3.8 mHz and 4.35–4.48 mHz
- Are induced by fast moving waves in the Earth's crust (for example, by Rayleigh waves propagating at about 3 km/s)
- Belong to acoustic branch of AGW dispersion relation
- Coupled to background vibrations in solid Earth

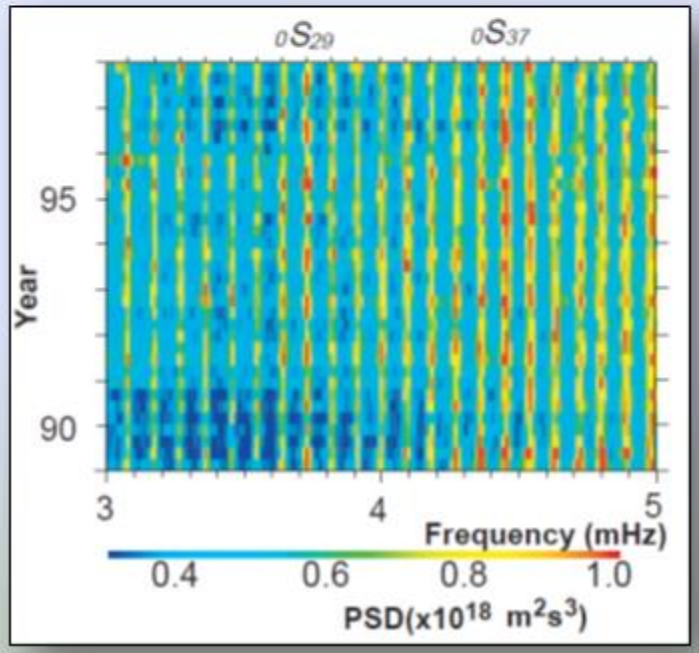

Amplitudes of the fundamental spheroidal modes averaged over all the available seismographic stations and over all the available days from 1989 to 1998. [Nishida K. et al., Science, 2000, Fig. 1]

Resonances in gravity waves radiated by the ocean

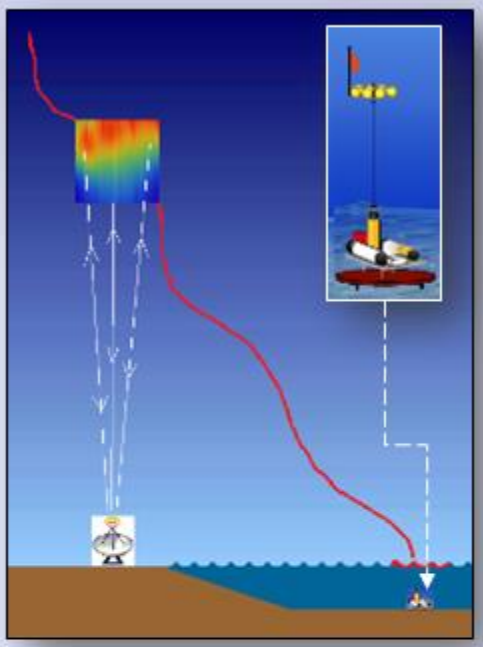

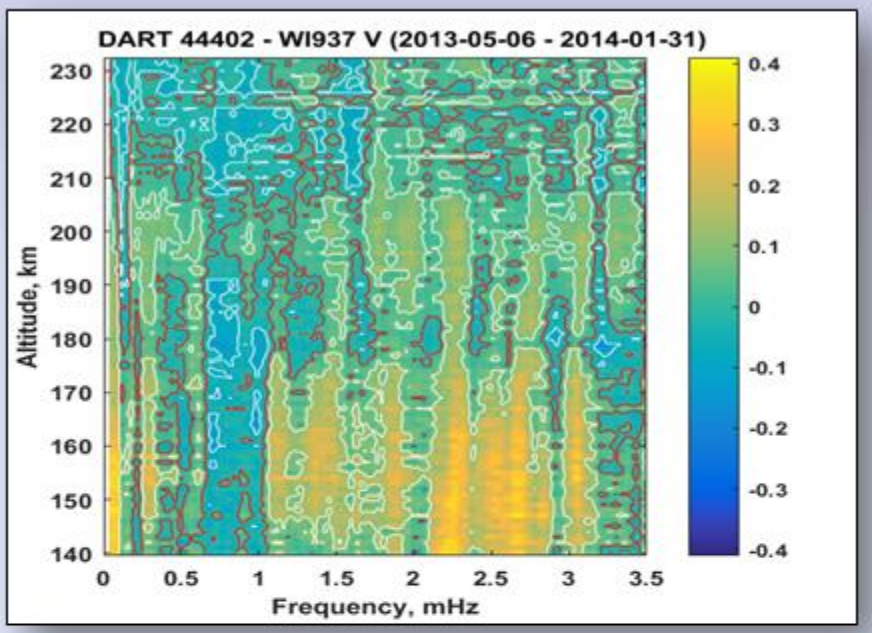

- Correlation of spectral amplitudes for thermospheric waves (Dynasonde) and infragravity waves (DART) shows frequency dependence
- 9 month long data series
- Every 1 km altitude range is processed individually
- 12-hour sliding time interval
- Lomb-Scargle spectral technique
- IGW-AGW correlation reaches 0.43

- Zabotin et al., *JGR Space Phys.*, 121, 2016; Godin et al., *Earth Planets Space*, 2015

Acoustic-gravity waves (AGWs) in the atmosphere

Background pressure and density:

$$p_0(z) = p_0(0)\exp\left(-\int_0^z \frac{dz}{h}\right) \qquad \rho(z) = \rho(0)\frac{h(0)}{h(z)}\exp\left(-\int_0^z \frac{dz}{h}\right)$$

Ideal gas:

$$c^2 = \frac{\gamma p_0}{\rho}, \quad h = \frac{c^2}{\gamma g}$$

AGW dispersion equation:

$$m^2 = \frac{\omega_d^2}{c_0^2} - k^2 + \frac{gk^2}{\omega_d^2}\left(\frac{1}{h} - \frac{g}{c_0^2}\right) - \frac{1}{4h^2}$$

Intrinsic frequency:

$$\omega_d = \omega - \mathbf{k}\cdot\mathbf{v}_0$$

Propagating waves:

$$\omega_d > \frac{\gamma g}{2c_0} \quad \text{or} \quad \omega_d^2 < N_0^2 = \frac{(\gamma-1)g^2}{c_0^2}$$

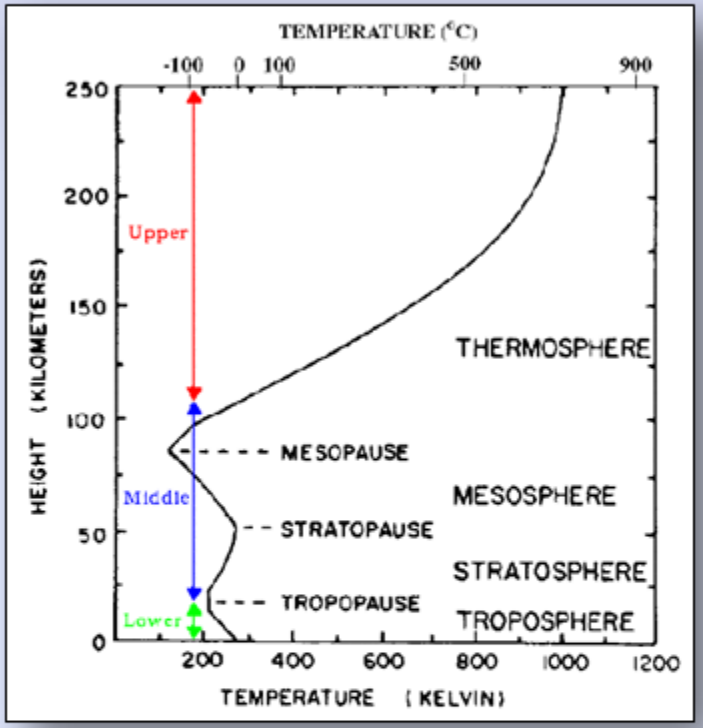

Dispersion equation of atmospheric waves on rotating Earth (f-plane approximation):

$$m^2 = \frac{\omega_d^2}{c_s^2} - \frac{\gamma^2 g^2}{4c_s^4} - \frac{\omega_d^2 k^2}{\omega_d^2 - f_c^2}\left[1 - \frac{(\gamma-1)g^2}{\omega_d^2 c_s^2}\right]$$

Coriolis parameter:

$$f_C = 4\pi T_e^{-1}\sin\theta$$

WKB approximation

First WKB approximation for AGWs:

$$p_L(z) = p_L(0)\sqrt{\frac{\rho m(0)\left(\omega_d^2 - g^2k^2/\omega_d^2\right)}{\rho(0)m\left[\omega_d^2(0) - g^2k^2/\omega_d^2(0)\right]}}\exp\left(i\mathbf{k}\cdot\mathbf{r} \pm i\int_0^z m dz_1 \pm i\chi\right)$$

Geometric, or Berry, phase:

$$\chi = \int_0^z \frac{dz_1}{2m}\left[\frac{gk^2}{\omega_d^2}\frac{d}{dz_1}\ln\left(\frac{h}{\omega_d^4 - g^2k^2}\right) + \frac{1}{2h}\frac{d}{dz_1}\ln\left(\frac{\omega_d^4 - g^2k^2}{\omega_d^4}\right)\right]$$

Lagrangian pressure perturbation:

$$p_L = p - \rho g w$$

Polarization relations:

$$w(z) = \frac{gk^2\omega_d^{-2} \pm im - 1/2h}{\left(\omega_d^2 - g^2k^2\omega_d^{-2}\right)\rho}p_L(z), \quad p(z) = \frac{\omega_d^2 \pm img - g/2h}{\omega_d^2 - g^2k^2\omega_d^{-2}}p_L(z)$$

Turning point:

$$m(z_t) = 0$$

First WKB approximation for acoustic waves:

$$p(z) = p(0)\sqrt{\frac{\rho\omega_d^2 m(0)}{\rho(0)\omega_d^2(0)m}}\exp\left(\pm i\int_0^z m dz_1\right), \quad m^2 = \frac{\omega_d^2}{c^2} - k^2$$

O. A. Godin, Wentzel–Kramers–Brillouin approximation for atmospheric waves, J. Fluid Mech. 777, 260–290 (2015); O. A. Godin, Diffraction of acoustic-gravity waves in the presence of a turning point, J. Acoust. Soc. Am. 140, 283–295 (2016)

Resonance excitation of atmospheric waves by ground surface vibrations

Boundary condition on a rigid surface z = 0:

$$w(z=0) = w_S$$

Vertical displacement of the ground surface:

$$w_S = w_0 \exp(i\xi x - i\omega t), \quad \xi = \omega / V$$

Turning point:

$$m(z_t) = 0$$

Resonance condition:

$$\varphi(z_t) + \chi(z_t) = \pi\left(n + \frac{1}{4}\right) - \arctan\left[\frac{g}{m(0)}\left(\frac{k^2}{\omega_d^2(0)} - \frac{\gamma}{2c^2(0)}\right)\right]$$

Response of the atmosphere to the plane-wave excitation:

$$W(\xi, z) = \sqrt{\frac{\rho_0 m_0\left(\omega_{d0}^2 - g^2k^2/\omega_{d0}^2\right)}{\rho m\left(\omega_d^2 - g^2k^2/\omega_d^2\right)}}\left[\frac{gk^2}{\omega_{d0}^2} - \frac{1}{2h_0} + im_0 - iB\left(\frac{gk^2}{\omega_{d0}^2} - \frac{1}{2h_0} - im_0\right)\right]^{-1}$$

$$\times\left\{e^{i\varphi(z)+i\chi(z)}\left(\frac{gk^2}{\omega_d^2} - \frac{1}{2h} + im\right) - iBe^{-i\varphi(z)-i\chi(z)}\left(\frac{gk^2}{\omega_d^2} - \frac{1}{2h} - im\right)\right\}, \quad B = e^{2i\varphi(z_t)+2i\chi(z_t)}$$

Finite source:

$$w_S = \int_{-\infty}^{\infty} \exp(i\xi x)\Phi(\xi)\, d\xi$$

AGWs due to the finite source:

$$w(z) = \int_{-\infty}^{\infty} \exp(i\xi x)\Phi(\xi) W(\xi, z)\, d\xi$$

Resonance contribution to the atmospheric response:

$$w_n(z) = \sqrt{\frac{\rho_0 m_0\left(\omega_{d0}^2 - g^2k^2/\omega_{d0}^2\right)}{\rho m\left(\omega_d^2 - g^2k^2/\omega_d^2\right)}}\frac{\Phi(\xi_n)}{D(\mathbf{k})} e^{i\xi_n x}\left[e^{i\varphi(z)+i\chi(z)}\left(\frac{gk^2}{\omega_d^2} - \frac{1}{2h} + im\right) - iBe^{-i\varphi(z)-i\chi(z)}\left(\frac{gk^2}{\omega_d^2} - \frac{1}{2h} - im\right)\right],$$

$$D = -\left(m_0 - i\frac{gk^2}{\omega_{d0}^2} + \frac{i}{2h_0}\right)\int_0^{z_t}\left\{\left[1 - \frac{(\gamma-1)g^2}{c^2\omega_d^2}\right]k + \left[1 - \frac{(\gamma-1)k^2g^2}{\omega_d^4}\right]\frac{u_x\omega_d}{c^2}\right\}\frac{dz}{m}$$

Dispersion relation for acoustic resonances

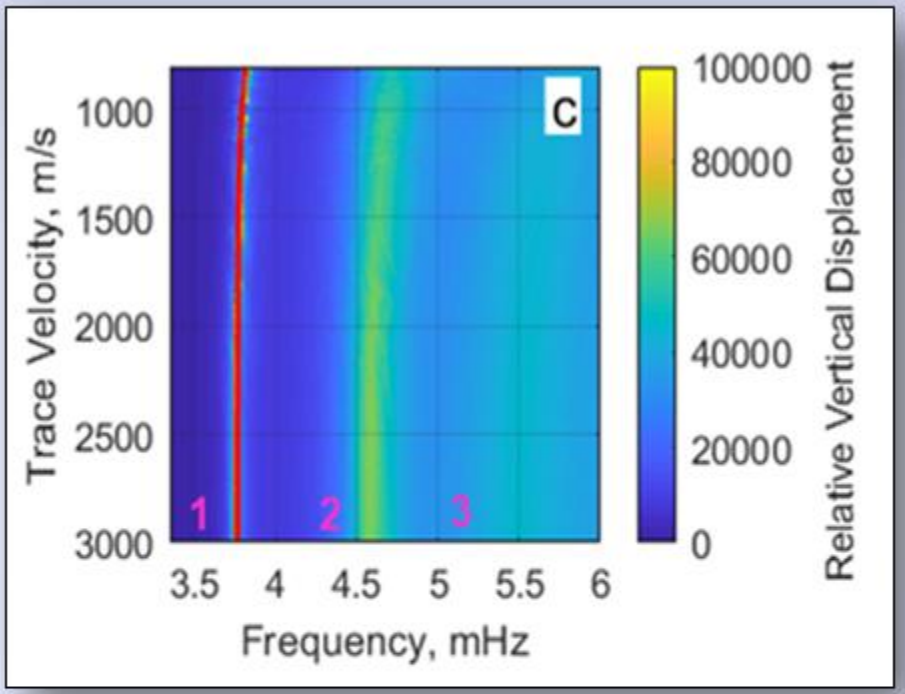

Variation of the resonance frequency and quality factor of acoustic resonances with the trace velocity of excitation. Color shows displacement amplitude at z = 180 km. The red line is the WKB predictions for the frequency of the first acoustic resonance. July 15 conditions over Wallops Island (Virginia, USA) are assumed in this simulation.

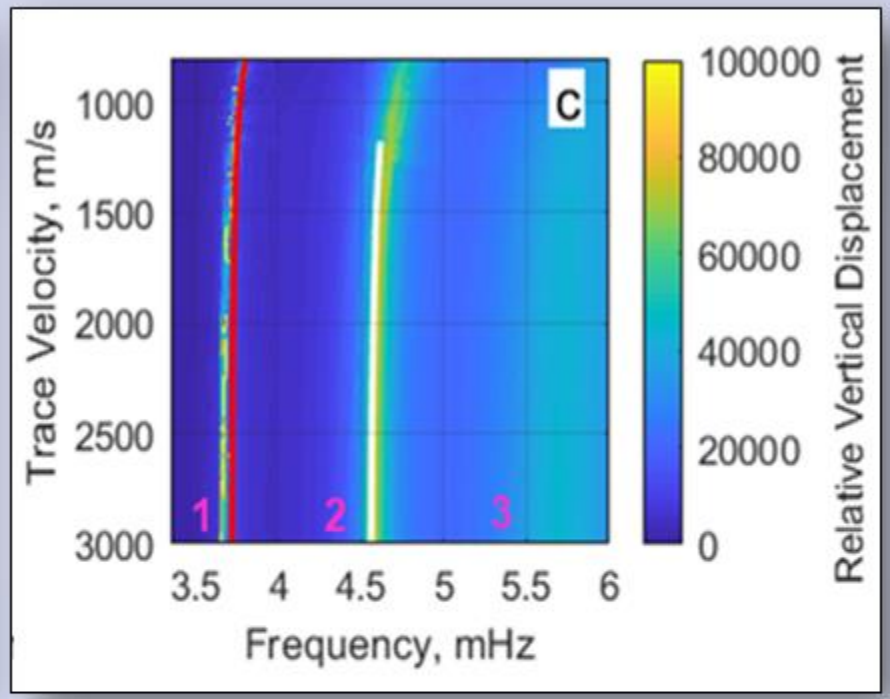

Same, but for July 15 conditions over McMurdo (Antarctica) are assumed in this simulation. The WKB predictions for the frequencies of the first and second acoustic resonances are shown by the red and white lines, respectively.

Environmental data are from NRLMSISE-00.2+HWM14, July 14

Resonant and non-resonant atmospheric response to monochromatic excitation at the ground level

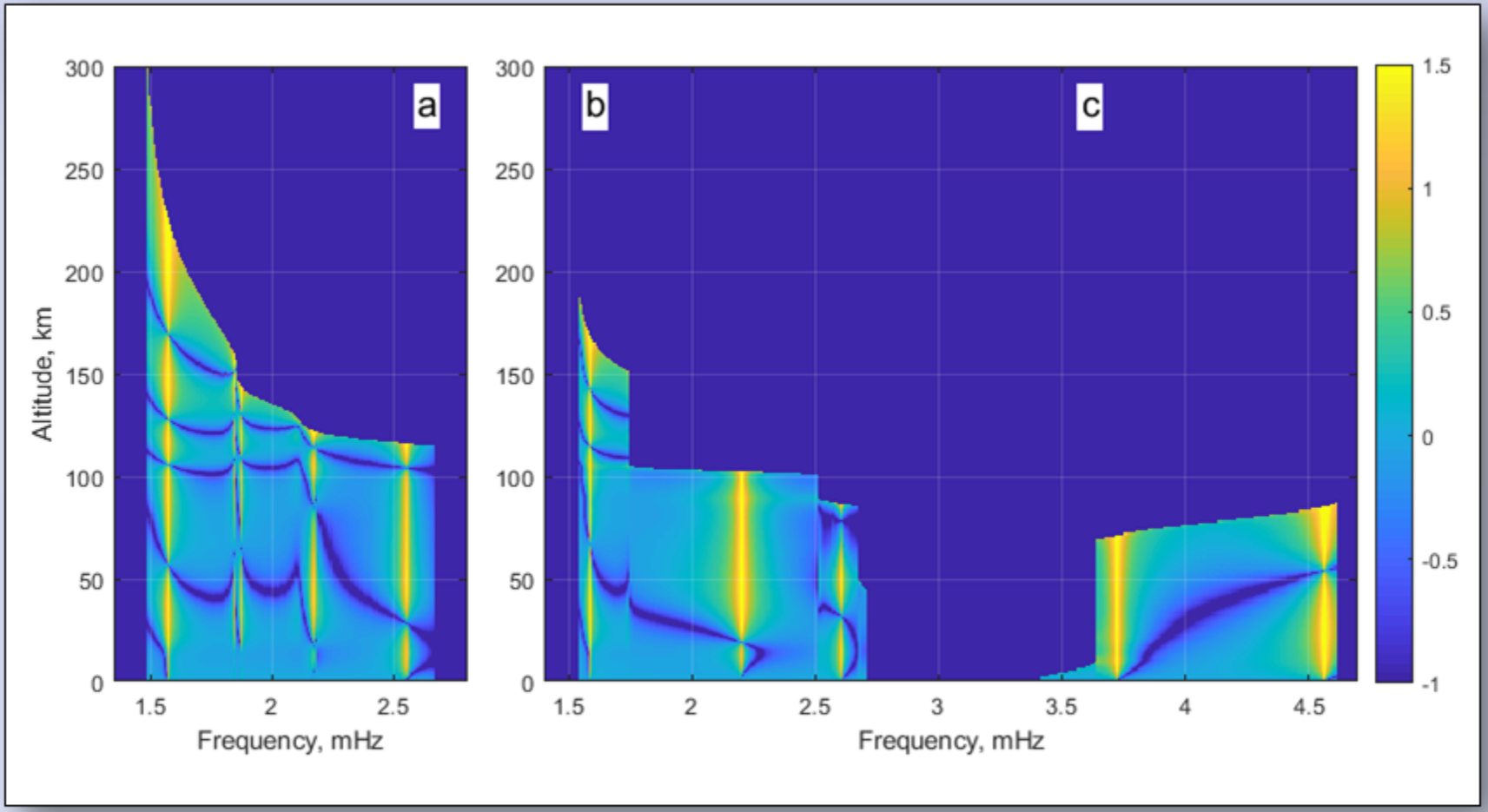

Response of the atmosphere to monochromatic vibrations of its lower boundary. The amplitude of the vertical displacement normalized by its value at the ground level is shown by logarithmic color scale, as a function of altitude and the frequency. Atmospheric waves are excited by vibrations that travel (a) westward and (b) eastward with subsonic trace velocity V = 200 m/s; and (c) southward at supersonic trace velocity V = 3000 m/s. Environmental data are from NRLMSISE-00.2+HWM14.

Propagation properties of buoyancy resonances in a mid-latitude atmosphere

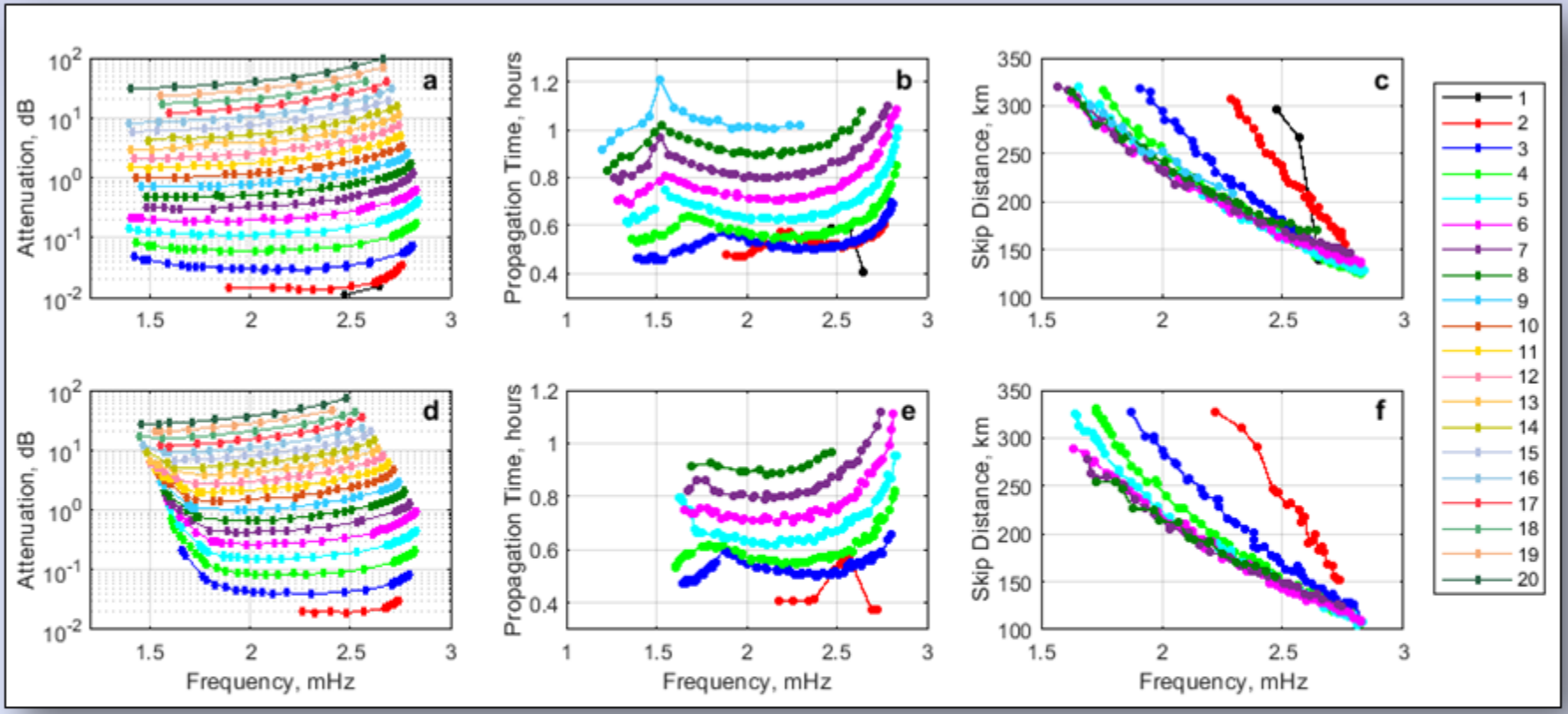

AGW attenuation (dB), travel time (h), and skip distance (km) in the ray approximation for atmospheric conditions at Wallops Island, Virginia, at GMT 06:00 (a – c) and GMT 18:00 (d – f) on 15 January 2014. Background temperature and wind velocity are from the NRLMSISE-00.2 and HWM14. Orders of the resonances are distinguished by color. (a), (d) Wave attenuation for resonances with n ≤ 20. (b), (e) and (c), (e) AGW propagation time and skip distance for the well-defined resonances with the attenuation not exceeding 1 dB.

Diversity of resonance conditions for gravity waves radiated by the ocean in mid latitudes

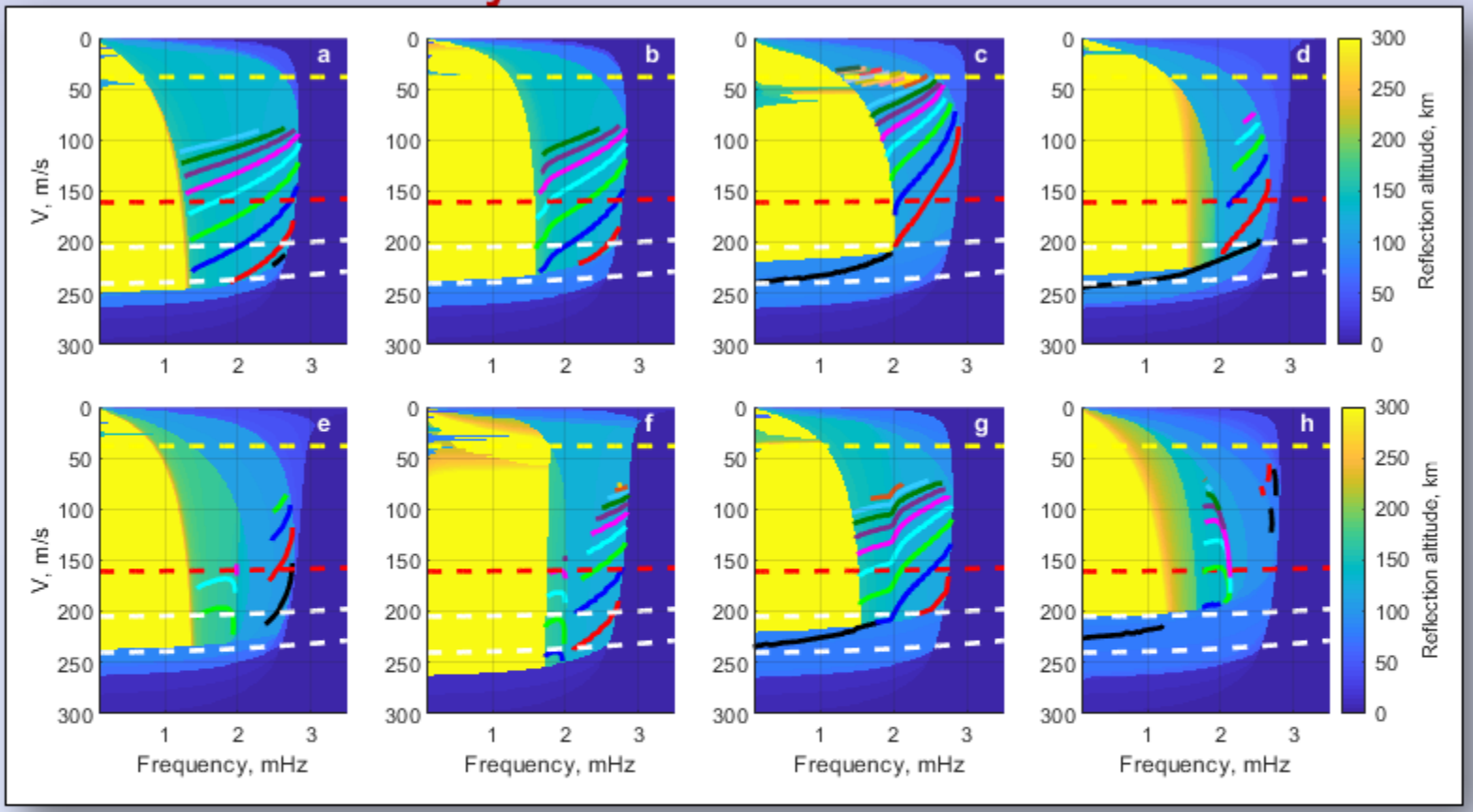

Well-defined buoyancy resonances with the attenuation not exceeding 1 dB are shown by solid lines, with color marking their order. Color scale represents the altitude of AGW turning point. The dashed lines show dispersion curves of infragravity waves in the ocean with depth of 150 m (yellow), 2649 m (red), 4300 m (top white) and 5900 m (bottom white). The background atmospheric parameters are for Wallops Island, Virginia for two specific dates: 15 January 2014 (a–d) and 14 July 2014 (e–h). For each date two times of the day, GMT 06:00 (a, c, e, g) and GMT 18:00 (b, d, f, h), and two directions of the wave propagation, eastward (a, b, e, f) and westward (c, d, g, h) are shown.

Full-wave solution confirms prediction of buoyancy resonances made with WKB approximation

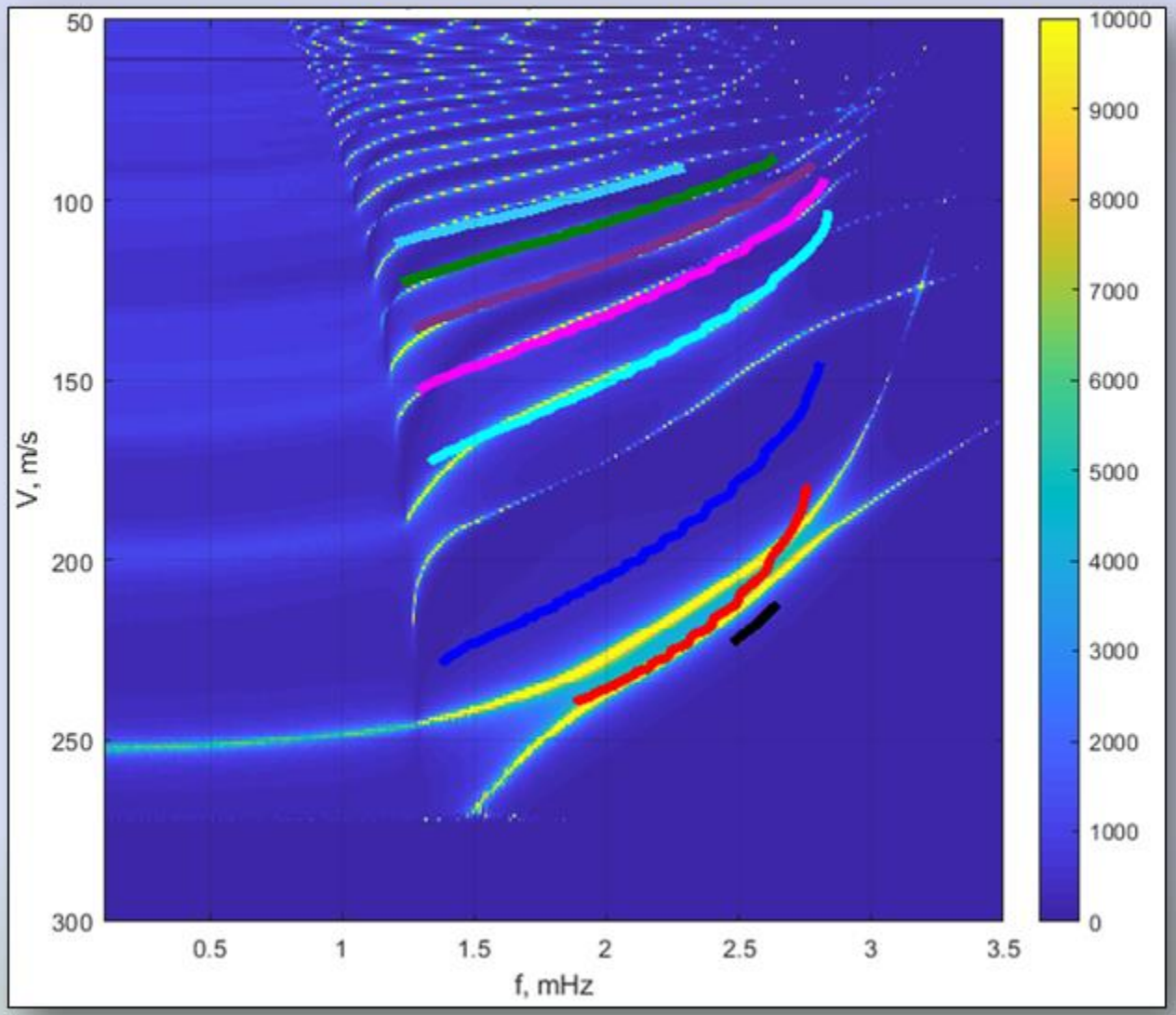

Color scale shows displacement amplitude resulting from the full-wave solution at z = 100 km.

Color lines correspond to well-defined resonances with the attenuation not exceeding 1 dB.

Environmental conditions are the same as for panel (a) in previous slide.

There is good correspondence between full-wave solution and WKB for resonances with n > 3.

Bathymetry of north-west Atlantic and correlation of the oceanic and atmospheric wave activity observed in the area

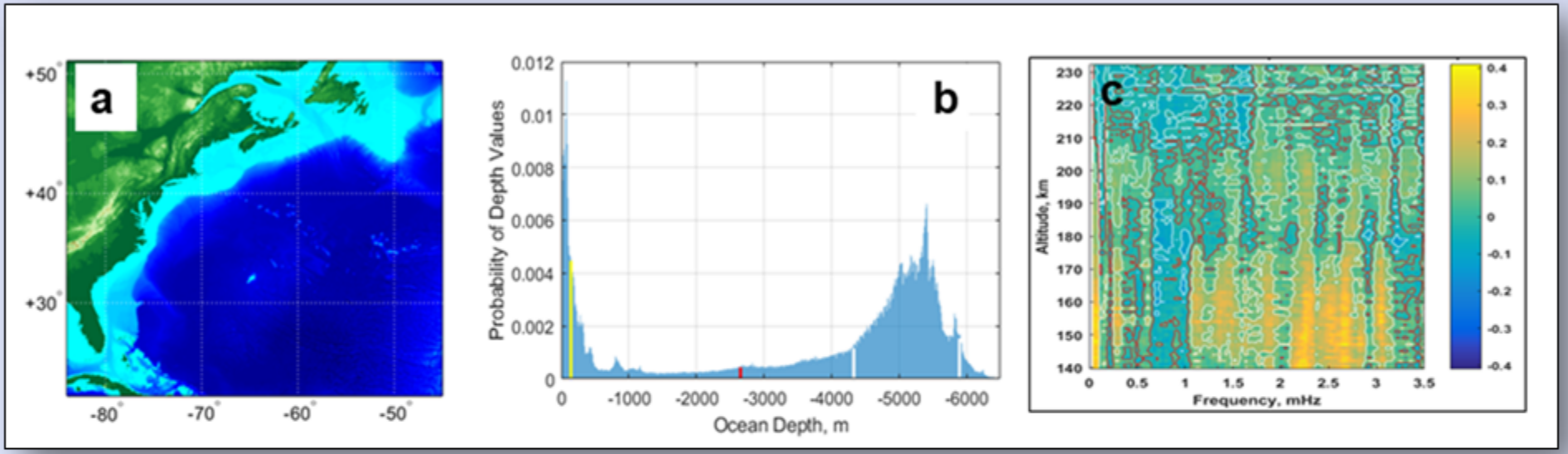

(a) Bathymetry map of north-west Atlantic. (b) Probability density function of water depths in the part of the Atlantic Ocean depicted in (a). Depth distribution is calculated using the satellite altimetry-derived global 2-minute bathymetry dataset. The four water depths indicated by color, 150 m (yellow), 2649 m (red), 4300 m and 5900 m (white), are the depths for which the infragravity wave dispersion curves are shown in previous slide. Correlation coefficient of spectral amplitudes of the wave activities observed in the Atlantic Ocean at the location of NDBC DART Station 44402 (39.30°N 70.66°W) and in the thermosphere over the Wallops Island, Virginia. [Panel (c) is adapted from Zabotin et al., 2016]

Conclusions

- The influence of specific propagation characteristics of the gravity waves (their oblique propagation and dissipative attenuation) on conditions of their observation has been investigated based on asymptotic (WKB, ray tracing) methods and a full wave equation.
- The strongest coupling of atmospheric waves to infragravity waves in the ocean is expected to occur when atmospheric resonances are excited.
- For many buoyancy resonances the gravity wave skip distance is shorter than horizontal dimensions of typical wave packets.
- The dissipative attenuation eliminates some of the resonance modes, but still many of them remain intact.
- Unlike acoustic resonances, buoyancy resonances are sensitive to wind velocity profiles and exhibit appreciable diurnal variation.
- Non-stationarity of the atmosphere is an important factor limiting possibilities to observe the buoyancy resonances. Nevertheless, relatively low threshold for meeting all other conditions for their appearance and temporal/geographical diversity of the atmosphere makes it still quite probable to see their manifestations.